12th International Conference on Advances in Steel-Concrete Composite Structures (ASCCS 2018)
Universitat Politècnica de València, València, Spain, June 27-29, 2018
Doi: http://dx.doi.org/10.4995/ASCCS2018.2018.6937

Tests on sea sand concrete-filled stainless steel tubular stub columns

F.Y. Liao[a]*, C. Hou[b], W.J. Zhang[a] and J. Ren[b]

[a]College of Transportation and Civil Engineering, Fujian Agriculture and Forestry University, P. R. China
[b]School of Civil Engineering, The University of Sydney, Australia
*corresponding author, e-mail address: feiyu.liao@fafu.edu.cn

Abstract

This paper presents a series of tests on sea sand concrete-filled stainless steel tubular (SSCFST) stub columns under axial compression, where the main test parameters include type of fine aggregates (river sand, desalted sea sand and sea sand), steel ratio, and concrete strength. The failure mode, axial load versus axial shorten response, cross-sectional strength of the SSCFST specimens are investigated and compared with those of traditional composite columns with normal concrete. The confinement effect between stainless tube and the sea sand concrete is also evaluated. High strength and good ductility was observed for the tested SSCFST stub columns. In general, when being used as the concrete core in a composite column, differences of confinement behaviour between sea sand concrete and normal concrete are not significant, indicating the potential adoption of SSCFST columns in practice.

Keywords: *Sea sand concrete; stainless steel; concrete-filled steel tube; stub column; cross-sectional strength; confinement effect.*

1. Introduction

With the aim of reducing the consumption of the river sand needed for making concrete mixture and advancing the sustainability of environment, sea sand can be adopted as an alternative aggregate in concrete mixture. However, the chloridion in sea sand might significantly aggravate the corrosion of structural steel. Therefore, materials with high corrosion resistance are required to apply with sea sand concrete, such as stainless steel. Recently, sea sand concrete-filled stainless steel tube has attracted expanding attention due to its environmentally friendly benefits [1, 2].

In the past, some experimental studies on concrete-filled stainless steel tubes were carried out by various researchers [3-7], however, the research on sea sand concrete-filled steel tubes is still not sufficient. Therefore, this paper conducted a series of tests on the sea sand concrete-filled stainless steel tubular (SSCFST) stub columns under axial compression. The failure mode, axial load versus axial displacement response, and ultimate strength of SSCFST stub columns were experimentally investigated, and the feasibility of using sea sand concrete to replace the river sand concrete in concrete-filled steel tube was examined.

2. Experimental program

2.1. Specimen preparations

A total of 24 circular concrete-filled stainless steel tubular (CFSST) stub columns were tested under axial compression. The main testing parameters are the type of fine aggregate (river sand, desalted sea sand, and sea sand), steel ratio, and concrete strength.

The information of all specimens is listed in Table 1, in which D is the overall diameter of steel tube, t is the wall thickness of tube, f_{cu} is the cubic strength of concrete, α ($=A_s/A_c$, where A_s is the cross sectional area of steel tube, A_c is the cross sectional area of core concrete) is the steel ratio, $\sigma_{0.2}$ is the 0.2% proof stress of stainless steel, ξ ($A_s f_y/A_c f_{ck}$, f_y is yield stress of the carbon steel; f_{ck} is the characteristic strength of the concrete, and the value of f_{ck} is determined using 67% of f_{cu} for normal strength concrete) is the confinement factor of concrete-filled steel tube. The lengths of specimens are all 480 mm.

2.2. Material properties

The cold-formed stainless steel tubes were cut and machined to the required length, and then were welded to a 30 mm thick steel base plate at one end. The measured modulus of elasticity (E_s), 0.2% proof stress ($\sigma_{0.2}$), ultimate strength (f_u), Poisson's ratio (v_s), and strain-hardening exponent of the stainless steel tube are presented in Table 2.

All the CFSST specimens were cast with one batch of self-consolidating concrete (SCC) without any vibration. Three types of sand were employed as the fine aggregates, i.e. river sand, desalted sea sand and sea sand, as shown in Fig. 1. The sea sand was obtained at the coast in Chang Le district of Fuzhou city of China. The desalted sea sand was produced by soaking the sea sand in water for 6 hours, and then filtering out the shells in the sand after the sand dried. The measured cubic strengths of concrete at the testing are listed in Table 1. The proportion of chloride in each type of sand was measured as 0.14% for sea sand, 0.06% for desalted sea sand and 0.006% for river sand, respectively.

Table 1. Specimen information.

No.	Specimen number	D (mm)	t (mm)	type of sand	f_{cu} (MPa)	α ($\times10^{-2}$)	$\sigma_{0.2}$ (MPa)	ξ	N_{ue} (kN)
1	C-3-L-RS-1	159	2.88		44.0	7.66	383.9	1.00	1263.6
2	C-3-L-RS-2	159	2.88		44.0	7.66	383.9	1.00	1322.2
3	C-3-H-RS-1	159	2.88		51.4	7.66	383.9	0.85	1348.7
4	C-3-H-RS-2	159	2.88	River	51.4	7.66	383.9	0.85	1315.6
5	C-4-L-RS-1	159	3.80	sand	44.0	10.29	400.7	1.40	1807.6
6	C-4-L-RS-2	159	3.80		44.0	10.29	400.7	1.40	1644.0
7	C-5-L-RS-1	159	4.50		44.0	12.36	401	1.68	1712.9
8	C-5-L-RS-2	159	4.50		44.0	12.36	401	1.68	1630.1
9	C-3-L-DS-1	159	2.88		43.3	7.66	383.9	1.01	1309.5
10	C-3-L-DS-2	159	2.88		43.3	7.66	383.9	1.01	1290.9
11	C-3-H-DS-1	159	2.88		58.7	7.66	383.9	0.75	1513.7
12	C-3-H-DS-2	159	2.88	Desalted	58.7	7.66	383.9	0.75	1551.6
13	C-4-L-DS-1	159	3.80	sea sand	43.3	10.29	400.7	1.42	1597.6
14	C-4-L-DS-2	159	3.80		43.3	10.29	400.7	1.42	1611.9
15	C-5-L-DS-1	159	4.50		43.3	12.36	401	1.71	1725.4
16	C-5-L-DS-2	159	4.50		43.3	12.36	401	1.71	1739.2
17	C-3-L-SS-1	159	2.88		42.2	7.66	383.9	1.04	1366.1
18	C-3-L-SS-2	159	2.88		42.2	7.66	383.9	1.04	1333.2
19	C-3-H-SS-1	159	2.88		52.4	7.66	383.9	0.84	1465.9
20	C-3-H-SS-2	159	2.88	Sea	52.4	7.66	383.9	0.84	1451.7
21	C-4-L-SS-1	159	3.80	sand	42.2	10.29	400.7	1.46	1642.4
22	C-4-L-SS-2	159	3.80		42.2	10.29	400.7	1.46	1647.8
23	C-5-L-SS-1	159	4.50		42.2	12.36	401	1.75	1745.8
24	C-5-L-SS-2	159	4.50		42.2	12.36	401	1.75	1715.0

Table 2. Material property of stainless steel.

$D\times t$ (mm)	$\sigma_{0.2}$ (MPa)	v	E_s (MPa)	n
159×2.88	383.9	0.27	195200	3.13
159×3.80	400.7	0.26	184433	5.07
159×4.50	401	0.27	177000	7.07

2.3. Test set up

The test set-up and instrumentation are shown in Fig. 2. A testing machine of 5000 kN capacity was used for the compression test. For each specimen, eight strain gauges were mounted on the outer surface of steel tube to measure the axial and transverse strain at mid-height of the column. Two displacement transducers were installed in the bottom to record the axial shortening. To obtain the softening response of the specimens, the loads were applied at closer intervals near the ultimate load.

Fig. 1. Three types of fine aggregate.

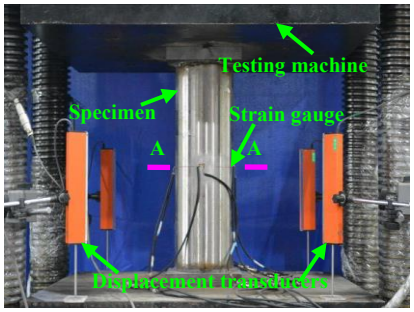

(a) Test setup.

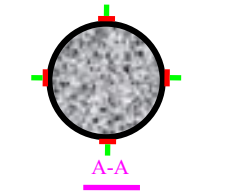

(b) Strain gauges.

Fig. 2. Testing set up and instrumentation.

3. Test results and discussions

3.1. Failure mode

All the tested specimens showed a local buckling failure mode, shown in Fig. 3. Due to the supporting effect of core concrete, only outward buckling of steel tube was observed in all CFSST specimens. The strain steel exhibits very good deformation ability, where no fracture was observed even under severe buckling conditions. In general, the effect of three types of sand on the failure mode is minor.

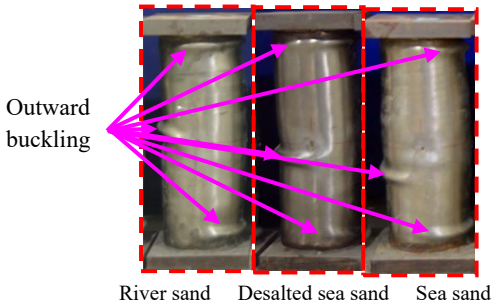

Fig. 3. Typical Failure modes of the CFSST specimens with different types of sand.

3.2. Axial load versus axial shorten curves

Fig. 4 shows the measured axial load (N) versus axial displacement (Δ) curves of the CFSST stub columns. At the initial loading stage, the N-Δ response shows the linear characteristic. With the yielding of steel tube, the curve gradually enters the elasto-plastic stage and shows nonlinear characteristic, where the stiffness tends to decrease.

Due to the strong confinement of the core concrete provided by the outer steel tube and the significant strain hardening feature of stainless steel, the CFSST specimen show very good ductility and deformation ability, where the N-Δ curve of all specimens has no descending stage and the axial load keeps rising until the end of testing. With the increase of wall thickness of steel tube, the hardening of N-Δ curve tends to be more marked. It also can be seen from Fig. 4 that, the replacement of sea sand for river sand has no significant effect on the N-Δ curve of CFSST stub column, because the confinement offered by the steel tube might eliminate the unfavorable influence caused by the shells in the sea sand.

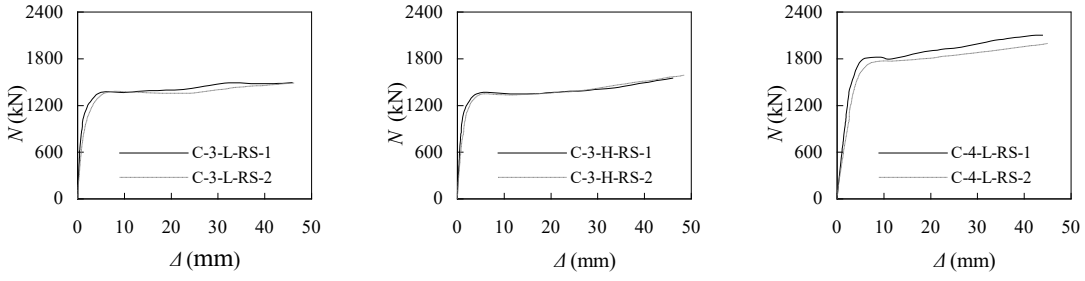

(a) C-3-L-RS (t=2.88mm, f_{cu}=44.0MPa, River sand)

(b) C-3-H-RS (t=2.88mm, f_{cu}=51.4MPa, River sand)

(c) C-4-L-RS (t=3.90mm, f_{cu}=44.0MPa, River sand)

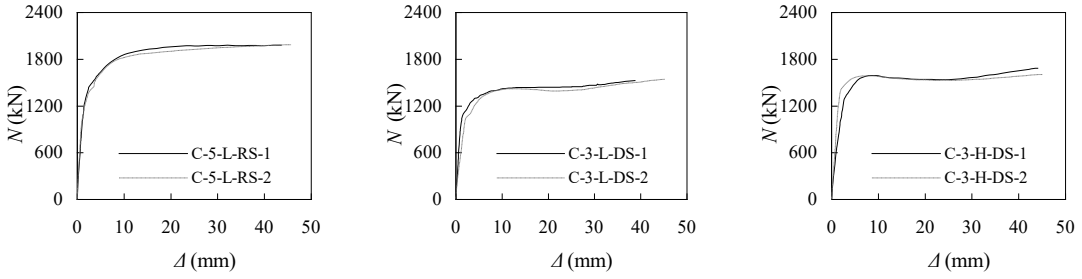

(d) C-5-L-RS (e) C-3-L-DS (f) C-4-H-DS

(t=4.50mm, f_{cu}=44.0MPa, River sand) (t=2.88mm, f_{cu}=43.3MPa, Desalted sea sand) (t=3.90mm, f_{cu}=43.3MPa, Desalted sea sand)

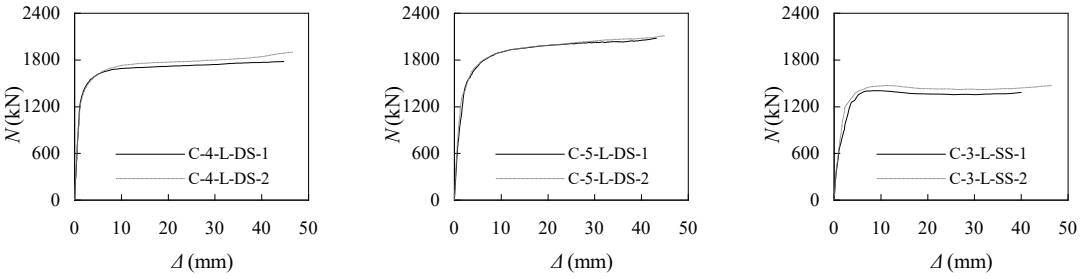

(g) C-4-L-DS (h) C-5-L-DS (i) C-3-L-SS

(t=3.90mm, f_{cu}=43.3MPa, Desalted sea sand) (t=4.50mm, f_{cu}=43.3MPa, Desalted sea sand) (t=2.88mm, f_{cu}=42.2MPa, Sea sand)

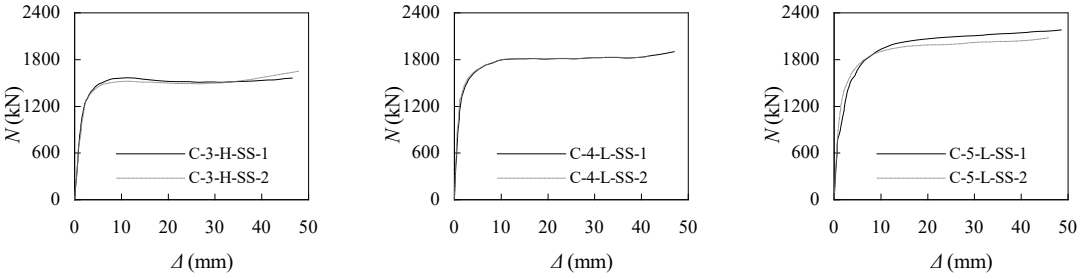

(j) C-3-H-SS (k) C-4-L-SS (l) C-5-L-SS

(t=2.88mm, f_{cu}=42.2MPa, Sea sand) (t=3.90mm, f_{cu}=42.2MPa, Sea sand) (t=4.5mm, f_{cu}=42.2MPa, Sea sand)

Fig. 4. Axial Load (N) versus axial displacement (Δ) curves.

3.3. Comparisons of ultimate strength

Fig. 5 compares the ultimate strength of tested specimens. Since the N-Δ of the specimen keeps ascending until the end of loading, the ultimate strength is defined in this paper as the axial load as the axial compressive strain reaches 10000 με. It is evident that the ultimate strength of CFSST columns tends to increase with the increase of steel ration, mainly due to the improved confinement effect of core concrete provided by the steel tube. For instance, as the steel ratio is increased from 7.66% to 12.36%, the ultimate strength of is improved by 29.2%, 33.2% and 28.2% respectively for the specimen infilled with river sand concrete, desalted sea sand concrete and sea sand concrete.

It is also found that, using different types of sand has a less significant influence on the ultimate strength of CFSST columns. Once again, the confinement effect of concrete largely contributes to such phenomenon by reducing the unfavourable effect of sea sand.

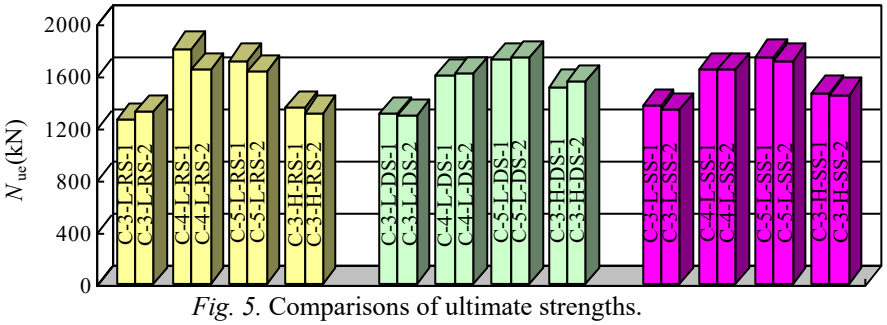

Fig. 5. Comparisons of ultimate strengths.

In order to quantitatively compare the confinement effect of the concrete with different types of fine aggregates, two strength indexes SI_1 and SI_s are defined as follows:

$$SI_1 = N_{ue}/(A_s\sigma_{0.2} + A_c f_{ck}) \quad (1)$$

$$SI_2 = SI_1/SI_{1-RS} \quad (2)$$

in which SI_1 is the ratio between the measured ultimate strength and the sum of the cross-sectional capacity of steel tube and core concrete. The value of SI_1 can generally reflect the degree of confinement. $SI_{1\text{-}RS}$ is the value of SI_1 of the control specimen with river sand concrete.

Fig. 6 compares the SI_2-value of the CFSST stub columns with different types of sand. It is evident that the SI_2 of sea sand concrete-filled stainless steel tubular columns is higher than that of composite columns with river sand concrete, which indicates the confinement of sea sand concrete is not weaker than that of river sand concrete in a concrete-filled steel tube (CFST). It also indicates that the replacement of sea sand concrete for river sand concrete in a CFST column may not have a significant effect on the ultimate strength of CFST columns.

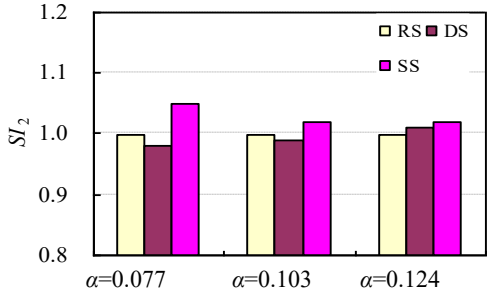

(a) Lower strength concrete

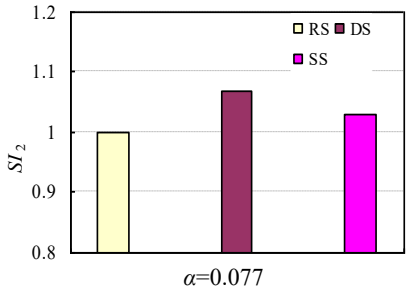

(b) Higher strength concrete

Fig. 6. Comparison of strength index SI_2

4. Conclusions

The following conclusions can be drawn within the scope of the current study:

(1) The tested sea sand concrete-filled steel tubular stub columns exhibits very good ductility and deformation ability.

(2) The effect of different types of fine aggregate is less significant on the failure mode and axial load versus axial displacement response.

(3) The replacement of sea sand concrete for river sand concrete will not weaken the confinement effect in a concrete-filled steel tubular column, which might indicate the feasibility of the application of sea sand concrete-filled steel tubes in practice.

Acknowledgments

The study of this paper is financially supported by the National Natural Science Foundation of China (51578154) and International Collaborative Funding of Fujian Agriculture and Forestry University (KXGH1700A). The financial support is highly appreciated.

References

[1] Li LY, Zhao XL, RamanSingh RK, Al-Saadi S. Tests on sea water and sea sand concrete-filled CFRP, BFRP and stainless steel tubular stub columns. Thin-walled Structures 2016; 108: 163-184.

[2] Li LY, Zhao XL, RamanSingh RK, Al-Saadi S. Experimental study on seawater and sea sand concrete-filled GFRP and stainless steel tubular stub columns. Thin-walled Structures 2016; 106: 390-406.

[3] Lam D, Gardner L. Structural design of stainless steel concrete-filled columns. Journal of Construction Steel Research 2008; 64: 1275-1282.

[4] Quach WM, Teng JG, Chung KF. Three-stage full-range stress-strain model for stainless steels. Journal of Structural Engineering 2008; 134: 1518-1527.

[5] Tam VW, Wang ZB, Tao Z. Behaviour of recycled aggregate concrete-filled stainless steel stub columns. Material and Structure 2014; 47: 293-310.

[6] Tao Z, Uy B, Liao FY, Han LH. Nonlinear analysis of concrete-filled square stainless steel stub columns under axial compression. Journal of Constructional Steel Research 2011; 67: 1719-1732.

[7] Uy B, Tao Z, Han, LH. Behaviour of short and slender concrete-filled stainless steel tubular columns. Journal of Constructional Steel Research 2011; 67: 360-378.